McGill 93-25
July 1993

A consistent next-to-leading-order QCD calculation of hadronic diffractive scattering

by

J.R. Cudell[†] and B.U. Nguyen[‡]

Department of Physics
McGill University
3600 University Street
Montréal, Québec, H3A 2T8, Canada

Abstract

We calculate the order α_s^2 and order α_s^3 QCD contributions to colour-singlet exchange in the leading $\log s$ approximation. We implement the resulting amplitude at the hadronic level and thus construct the QCD pomeron and odderon to this order of perturbation theory. We show that the structure of the hadronic form factors provides a natural mechanism through which the odderon gets suppressed at $t = 0$ whereas it dominates the elastic cross section at large t. We also demonstrate that the inclusion of nonperturbative effects through a modification of the gluon propagator accelerates greatly the convergence of the $\log s$ expansion, although not enough to provide agreement with the data.

[†]cudell@hep.physics.mcgill.ca
[‡]bao@hep.physics.mcgill.ca

1. Introduction

Hadronic diffractive scattering has defied theoretical understanding for the past twenty years. Although the data can be fitted remarkably well to a form that was predicted by the old Regge theory [1], perturbative QCD does not give rise to a pomeron and an odderon which agree with data. What perturbative QCD gives us instead is the so-called "perturbative pomeron", which seems to be a theoretical construct in need of experimental confirmation.

This "perturbative pomeron" results from the formidable machinery of the Balitskii-Fadin-Kuraev-Lipatov (BFKL) equation [2], and has the following drawbacks:
• Its leading contribution to the hadronic amplitude, for fixed α_s goes like $s^{1+12\log(2)\alpha_s/\pi}$, *i.e.* for any reasonable value of α_s, it increases much faster than the data, which behave like $s^{1.08}$ [1].
• At nonzero t, the differential elastic cross section has the wrong shape: its logarithmic slope at $t = 0$ is infinite and its curvature is too big.
• A more subtle problem stems from the fact that the pomeron-hadron vertex is almost local, *i.e.* similar to a photon exchange term, with the spin structure γ^μ. This property is necessary to reproduce the factorizability of the pomeron amplitudes [3]. QCD exchanges do not reduce to an effective photon-like interaction. The quark-quark interaction does, but the problem comes from the implementation of quark-quark scattering inside a hadron. Quark-quark scattering is infrared divergent. However, we know that colour-singlet objects do not interact at infinite distances. So the wavefunction effects have to cancel the infrared divergence. Unfortunately, the side-effect of this cancellation is to destroy the factorizability of a simple γ^μ vertex [4].

Another perturbative construct is the odderon. Although we shall not be able to evaluate its intercept at this order, we shall be able to tackle the following problem: experimentally, the "Landshoff term" [5], which arises from 3-gluon exchange, each gluon being attached to a different quark, gives the leading contribution to the elastic cross section at large t. However, we know that at small t, this odderon contribution is small. We shall explain how this feature emerges naturally for the lowest-order odderon.

Thus the three main questions we want to answer are the following: how can we reduce the intercept of the QCD pomeron? how can we limit the effects of the wave function? Why is the odderon negligible at small t and dominant at high t? Rather than trying to settle these issues through the BFKL equation [6], we shall perform a complete third-

order calculation (which is the first order at which one can see the pomeron intercept and slope) of hadron-hadron scattering. We shall show that all the problems of the leading-log resummation are present at this order of perturbation theory, and we shall think of it as a first-order Taylor expansion of $As^{\alpha_0+\alpha' t}$ in $\log s$. We can then directly use it as a laboratory in which we can test some of the ideas that have been proposed to resolve these puzzles.

The first class of ideas is to limit the wave function effects by assuming that the dynamics of the QCD vacuum provides an intrinsic infrared regulator. This idea was proposed by Landshoff and Nachtmann [7], who used an *ad hoc* form for the gluon propagator that enabled them to perform the required integrals. Since then, the infrared properties of the gluon propagator have been re-evaluated from a more theoretical point of view: solutions to the Dyson-Schwinger equation for the gluon propagator have indeed been found, solutions which are smoother than a pole in the infrared region [8, 9]. Also, some earlier work has proposed that the gluon develops a mass at zero momentum transfer [10]. We shall show here that the perturbative calculation can be easily recast in a form which allows for a modification of the gluon propagator, provided that there exists a Källen-Lehmann density: the complete third-order result then depends only on the t-channel propagators.

The second possibility is to study the form factors more closely. The calculation will involve two form factors in the pomeron case, and an extra one in the odderon case. One can either make a model for those, which will depend on an explicit proton wavefunction, or assume a simple parametrization. We shall pursue both routes.

The paper is organized as follows: in the second section, we re-examine the two-gluon calculation, set up most of the formalism and discuss the use of nonperturbative propagators at this order. The third section details the calculation of the amplitude to order α_s^3, first in the odderon case, then in the pomeron case. The fourth section is devoted to a discussion of our results. Note that we shall work in the Feynman gauge throughout.

2. Two-gluon exchange

Since the work of Low and Nussinov [11], it has been realized that the lowest-order QCD exchange that has the quantum numbers of the pomeron (charge parity $C = +1$, colour singlet) is two-gluon exchange.

As QCD is a theory of quarks and gluons, we must first consider quark-quark scattering. The lowest-order diagrams contributing to colour-singlet exchange are shown in Figure 1.

The two incoming quarks have momenta p^a and p^b, which, in the limit $s \approx 2\, p^a \cdot p^b \to \infty$, can be identified with the + and − directions of light-cone kinematics ($p_+ = p_0 + p_3$ and $p_- = p_0 - p_3$). If we consider elastic scattering, both the initial-state and the final-state quarks have to be near shell. That means that the momentum transfer $t = \Delta^2$ must be in the transverse direction, $\Delta \approx (0, \vec{\Delta}, 0)$ so that both $(p^a + \Delta)^2$ and $(p^b - \Delta)^2$ remain small as $s \to \infty$. (From now on, we shall denote the transverse direction by an arrow.)

In two-gluon exchange, the momentum kick Δ is split into two gluons $\Delta = k^a + k^b$. The diagrams of Figure 1 involve integrals of the form:

$$\int dk_+^a dk_-^a d\vec{k}_a \frac{s^2}{[(p^a - k^a)^2 - m^2]\,[(p^b + k^a)^2 - m^2]\,[(k^a)^2]\,[(\Delta - k^a)^2]} \tag{2.1}$$

The leading contribution comes from the region when one (and only one) of the quark propagators is of the order of s. This happens if the gluons carry a large component either in the + or in the − direction. The amplitude then contains a factor *e.g.* $\int dk_-^a/(p_+^a k_-^a) \approx (\log s)/s$. However, as $u \approx -s$, crossing symmetry implies that one graph behaves as $s \log s$ and the other as $-s \log(-s)$. Thus the two real parts cancel, leaving only an imaginary part.

In order to calculate this imaginary part, we can use cutting rules: in graph 1(a) we put the intermediate quarks on-shell, replacing their propagators by a delta function of their 4-momentum squared. The k_-^a and k_+^a integrals can then be done trivially, and bring a factor $1/s$. The same argument as for Δ holds, and the gluons have to be transverse: $k^a \approx \vec{k}_a$, $k^b \approx \vec{k}_b$.

To sum up, two-gluon exchange takes the following form:

$$\mathcal{A}_2^q(s,t) = i\alpha_s^2 s C_2 \int d\vec{k}_a d\vec{k}_b \frac{d\mathcal{A}_2^q}{d\vec{k}_a d\vec{k}_b} \tag{2.2}$$

with

$$\frac{d\mathcal{A}_2^q}{d\vec{k}_a d\vec{k}_b} = \delta^{(2)}(\vec{\Delta} - \vec{k}_a - \vec{k}_b) \frac{1}{(\vec{k}_a^2 + \sigma_a)} \times \frac{1}{(\vec{k}_b^2 + \sigma_b)} \tag{2.3}$$

where we have introduced two gluon squared masses σ_a and σ_b, which for now can be considered as infrared regulators, and a colour factor $C_2 = 8/9$.

2.1. Photon-photon scattering

Quark-quark scattering lacks a crucial property of hadron-hadron scattering: as their wavelength increases, one expects that gluon interactions will average out the colour of the

hadron, and thus effectively decouple. In other words, the calculation should be infrared finite. To verify this fact, we need a model for a hadron.

The simplest object for which the above argument holds is a photon, and since the work of Cheng and Wu, and Frolov, Gribov and Lipatov [12], it is known that the photon-photon scattering amplitude takes the form:

$$\mathcal{A}_2 \sim is \int d\vec{k}_a d\vec{k}_b \; \frac{d\mathcal{A}_2^q}{d\vec{k}_a d\vec{k}_b} [\mathcal{E}_1^\gamma(\vec{\Delta}^2) - \mathcal{E}_2^\gamma(\vec{k}_a, \vec{k}_b)]^2 \tag{2.4}$$

$\mathcal{E}_1^\gamma$ comes from graphs where the gluons are attached to the same quark line, see Figure 2(a), and takes the following form:

$$\mathcal{E}_1^\gamma(\vec{\Delta}^2) = 4\alpha_{em} \int_0^1 d\beta \int d\vec{p}\; \psi^*(\beta, \vec{p} + \frac{\beta\vec{\Delta}}{2}) \psi(\beta, \vec{p} - \frac{\beta\vec{\Delta}}{2}) \tag{2.5}$$

$\psi(\beta, \vec{p})$ is the wavefunction of a quark produced out of the photon with longitudinal momentum fraction β and transverse momentum $\vec{p}$. It can be shown to be:

$$\psi(\beta, \vec{p}) \sim \frac{\sqrt{\beta(1-\beta)}}{\vec{p}^2} \mathcal{P}_{ij}(\vec{p}, s) \tag{2.6}$$

with $\mathcal{P}_{ij}(\vec{p}, s)$ a factor that depends on the polarizations of the incoming and outgoing photons. $\mathcal{E}_2^\gamma$ comes from diagrams where the gluons are attached to different quark lines. For instance, Figure 2(b) will produce a term $\mathcal{E}_1^\gamma \mathcal{E}_2^\gamma$ in Eq. (2.4). This form factor can be written:

$$\mathcal{E}_2^\gamma(\vec{k}_a, \vec{k}_b) = \mathcal{E}_1^\gamma \left((\vec{k}_b(1/\beta - 1) - \vec{k}_a)^2 \right) \tag{2.7}$$

The important lesson is that $[\mathcal{E}_1(\vec{\Delta}^2) - \mathcal{E}_2(\vec{k}_a, \vec{k}_b)]^2 \sim \vec{k}_a^2$ as $\vec{k}_a \to 0$ (and similarly for $\vec{k}_b$), *i.e.* the infrared divergence of the gluon propagator is cancelled by the form factor. Also, the particular form taken by $\mathcal{E}_2^\gamma$ comes from the symmetry of the vertex $\gamma \to q\bar{q}$, which dictates for instance that $\psi(\beta, \vec{p}) = \psi(1-\beta, \vec{p})$. This property must be conserved in the pion case, but need not be present in the baryon case.

2.2. Hadron-hadron scattering

The preceeding formalism finds a natural extension in the work of Gunion and Soper [13]. Here and in the following, we shall assume that hadrons are composed of their valence quarks only. This amounts to saying that sea partons are generated by higher-order corrections.

In the high-s limit, the two incoming hadrons are living on the light-cone, *i.e.* at fixed x_- or x_+. These two directions then alternatively play the role of time in the definition of the wavefunctions ψ. Transforming the remaining free + or − components to momentum space, hadrons are thus described by a wavefunction $\psi(\{\beta_j\},\{\vec{r}_j\})$, with β_j the longitudinal momentum fraction of quark j and $\vec{r}_j$ its impact parameter in the center-of-momentum frame of the hadron. This wavefunction is a priori unknown. One can then show, in the eikonal approximation, that multi-gluon exchange takes the following form [13]:

$$\begin{aligned}\mathcal{A}_\infty &= -2is\int d\vec{b}e^{-i\vec{\Delta}.\vec{b}} \\ &\times \Big[\prod_{j=1,n_q}\int_0^1 d\beta'_j\int d\vec{r}_j\Big]|\psi(\beta'_j,\vec{r}_j)|^2\Big[\prod_{l=1,n_q}\int_0^1 d\beta_l\int d\vec{s}_l\Big]|\psi(\beta_l,\vec{s}_l)|^2 \\ &\times \left(exp\left(-i2\pi\alpha_s\sum_{i,j}\sum_{c=1,8}\lambda_i^c\lambda_j^c V(\vec{x}_i-\vec{x}_j)\right)-1\right)\end{aligned} \tag{2.8}$$

with

$$V(\vec{x}) = -\int dx^+dx^-\Delta_F(x^+,x^-,\vec{x}) \tag{2.9}$$

where one implicitly assumes an ordering of the vertices in the + and − directions. The key issue for this eikonal formula to be valid is that the scattering of the quarks lying at fixed p^- (respectively p^+) must not give final state quarks with a substantial + (resp. -) component, so that they can recombine into hadrons. More precisely, this "opposite" component must be of the order of $1/s$. As we shall see later, large rapidity gaps imply that some of the diagrams are suppressed for this reason, and we will have to subtract their contribution from expression (2.8). As from the argument leading to Eq. (2.2), large rapidity gaps do not contribute to two-gluon exchange, we shall not pursue the matter further here.

The eikonal formula for the scattering of two hadrons h_1 and h_2 containing n_1 and n_2 valence quarks via the exchange of two gluons is obtained by expanding Eq. (2.8) to order α_s^2. This gives:

$$\mathcal{A}_2 = i\alpha_s^2 sC_2n_1n_2\int d\vec{k}_a d\vec{k}_b\frac{d\mathcal{A}_2^q}{d\vec{k}_a d\vec{k}_b}[\mathcal{E}_1^{h_1}(\vec{k}_a+\vec{k}_b)-\mathcal{E}_2^{h_1}(\vec{k}_a,\vec{k}_b)][\mathcal{E}_1^{h_2}(\vec{k}_a+\vec{k}_b)-\mathcal{E}_2^{h_2}(\vec{k}_a,\vec{k}_b)] \tag{2.10}$$

$$\mathcal{E}_1(\vec{\Delta}) = \int d\mathcal{M}e^{i\vec{\Delta}.\vec{r}_k} \tag{2.11}$$

and

$$\mathcal{E}_2(\vec{k}_a,\vec{k}_b) = \int d\mathcal{M}e^{i\vec{k}_a.\vec{r}_k+i\vec{k}_b.\vec{r}_l} \tag{2.12}$$

with $l \neq k$. The natural integration measure $d\mathcal{M}$ is defined as:

$$d\mathcal{M} = [\prod_{j=1,n_q} d\beta_j d\vec{r}_j]\delta^{(2)}(\sum_j \beta_j \vec{r}_j)\delta(\sum_j \beta_j - 1)|\psi(\beta_j, \vec{r}_j)|^2 \tag{2.13}$$

The first delta function defines the center of momentum of the hadron, whereas the second one enforces longitudinal momentum conservation. Assuming that hadrons are made of valence quarks only, we normalize the wavefunction according to:

$$\int d\mathcal{M} = 1 \tag{2.14}$$

The same model applied to γp elastic scattering leads to the identification of $\mathcal{E}_1$ with the Dirac elastic form factor F_1. $\mathcal{E}_1$ is thus measured directly so that we know its form from experiment. In the proton case, we shall use a dipole electric form factor $G_E = (1 - t/0.71)^{-2}$, which fits the data to $t = 10$ GeV^2 at least [14]. This leads to the Dirac form factor:

$$\mathcal{E}_1(t) = \frac{(3.53 - 2.79t)}{(3.53 - t)\,(1 - t/0.71)^2} \tag{2.15}$$

In the pion case, the form factor has been measured only to moderate values of $t < 0.3$ GeV^2, so that we have to assume the functional form:

$$\mathcal{E}_1(t) = \frac{1}{(1 - t\ < r_\pi^2 > /6)} \tag{2.16}$$

where $\sqrt{< r_\pi^2 >} = 0.663$ fm is the electromagnetic radius of the pion [15].

The form of $\mathcal{E}_2$ is more arbitrary as the only firm property that can be established from Eq. (2.12) is the cancellation of the infrared divergences as $\vec{k}_a$ or $\vec{k}_b \to 0$, *i.e.* $\mathcal{E}_1 \to \mathcal{E}_2$. For the purpose of the present analysis, we adopt two strategies. The first is to allow $\mathcal{E}_2$ to vary according to a functional form guaranteeing infrared finiteness:

$$\mathcal{E}_2(\vec{k}_a, \vec{k}_b) = \mathcal{E}_1(\vec{k}_a^2 + \vec{k}_b^2 - f\vec{k}_a.\vec{k}_b) \tag{2.17}$$

The appropriate values in the pion case is $f = 2$ and in the proton case $f = 1$, corresponding to a wavefunction peaked at $\beta = 1/2$, and $\beta = 1/3$ respectively. The fact that $f = 2$ in the pion case is obvious: if both quarks are deflected by an identical amount in the transverse direction, and if their longitudinal momenta are equal, then they must recombine into a pion:

$$\mathcal{E}_2^\pi(\vec{k}, \vec{k}) = 1 \tag{2.18}$$

The parametrization (2.17) of the pion form factor, together with the value $f = 2$, result from the symmetry property (2.7), transposed to the case of a pion at fixed $\beta = 1/2$. We shall see in section 3.2 why f must be equal to 1 in the proton case †.

†In refs. [8, 16], the value $f = 7$ was erroneously used for proton-proton scattering.

The second strategy is to choose an explicit form for the hadron wavefunction. Assuming that the longitudinal momentum is distributed as in the valence quark structure function, we use:

$$\psi_{abc}(\{\vec{r}_i\},\{\beta_i\}) = N\epsilon_{abc}/\sqrt{6}\left(\prod_{i=1,3}\frac{(1-\beta_i)^n}{\sqrt{\beta_i}}\right)\times\exp\left(\frac{\sum_i \vec{r}_i^{\,2}}{r_h^2}\right) \qquad (2.19)$$

with N a normalization factor, $n = 3$ for protons and 1 for pions, r_h a hadronic radius and abc the colour of the quarks.

As can be seen from Figure 3, this form reproduces well the parametrization (2.15) for $r_p = 0.65\ fm$ while producing a physical model for $\mathcal{E}_2$. Note that for moderate values of $|\vec{k}_a|$, $|\vec{k}_b|$ the effect of the smearing of β is to shift f in Eq. (2.17), to $f \approx 0.8$ in the proton case and $f \approx 1.5$ in the pion case.

We give in Table 1 the results of perturbative two-gluon exchange. We have considered the calculation either at fixed α_s, or for a running $\alpha_s(q^2) = (12\pi/27)\log(q^2/\Lambda^2_{QCD})$, which we freeze once it gets to $\alpha_s = 1$. (We have taken $\Lambda^{(3)}_{QCD} = 0.3$ GeV, and assumed that the scale of α_s is the virtuality of the gluon attached at the vertex.) We also show the dependence of some of the results on our choice of form factor: the numbers in parenthesis are obtained using the model (2.19) for the proton wavefunction, and the others correspond to the simple parametrization (2.15- 2.17), both in the case of a fixed and of a running α_s.

Two-gluon exchange sets the scale correctly: the pp cross section is about $76\alpha_s^2$ mb, which for $\alpha_s \sim 0.5 - 1$ is of the right order of magnitude. Furthermore, the quark counting rule can be reproduced only if we assume that the $\mathcal{E}_1 - \mathcal{E}_2$ factors are not too different when going from the proton to the pion. If we use the form (2.17) with f=2 for pions and f=1 for protons, it turns out that the ratio $\sigma_{p\pi}/\sigma_{pp} = 0.65$ is close to the experimental number 0.62. Let us point out however that this is very sensitive to our input value for $< r_\pi^2 >$, and to the assumed functional dependence of Eq. (2.16). In perturbative QCD, the quark counting rule would then be only an accident, and the factorizability of the pomeron exchange [3] would be lost. However, the main problem comes from the elastic differential cross section. Its shape, as shown in Figure 4, comes out wrong: instead of an exponential, it has too much curvature, and its logarithmic slope at the origin turns out to be infinite.

These problems can be traced to the infrared region. To make this point clear, we show in Figure 5 the average momentum $k_{ave} =< |\vec{k}_a| >$ in formula (2.10) as a function of t. We see that it increases with $-t$, from a fraction of a GeV near $t = 0$ to about 1.5 GeV near $t = -10$ GeV^2. This means that even at high $-t$ the small-k^2 region will dominate: the truly perturbative region plays a negligible role in diffractive scattering. This feature

is identical at order α_s^3. It is thus important to examine this region in detail, and to see how the most modest changes in the infrared region can affect our results.

2.3. Nonpertubative effects

Landshoff and Nachtmann [7] have argued that a modification of the gluon propagator can produce a factorizing amplitude, which in turn should remove the wavefunction dependence, restore factorization, and make $B(0)$ finite.

In order to use a modified gluon propagator, we must first observe that the infrared regulators of formulae (2.2) can be treated as the squared masses that enter the Källen-Lehmann representation for the propagator:

$$D(q^2) = \int_0^\infty d\sigma \frac{\rho(\sigma)}{q^2 - \sigma + i\epsilon} \tag{2.20}$$

Note that in fact we do not need a Källen-Lehmann density *per se*, but simply the existence of a Hilbert transform, i.e. neither the range of integration nor the reality of ρ will matter in the following.

One can then repeat the perturbative calculation by commuting the σ integrals and the d^4k integrals. One obtains the same results (2.2, 2.3, 2.4), which then need to be convoluted with the Källen-Lehmann densities $\rho(\sigma_1)$, $\rho(\sigma_2)$. This reconstructs the propagators, and the $\frac{1}{k^2+\sigma}$ then becomes $-D(-k^2)$ because of Eq. (2.20).

We shall see that this property of the amplitude is encountered again at the next order of perturbation theory: the perturbative propagators can be replaced by nonperturbative ones, and provided that there exists a Hilbert transform, we can justify this substitution on theoretical grounds.

One might however still worry about the gauge invariance of the theory: if the structure of the QCD vacuum changes the propagators, then in order to obey the Ward-Slavnov-Taylor (WST) identities, the vertices need to be modified, and probably the quark propagators, too. As far as the vertices go, one can argue that if the Källen-Lehmann density $\rho(\sigma)$ is concentrated near the origin, then the corrections to the vertices are probably of the order of σ, and thus these contributions are going to be small (this is confirmed by the results of Ref. [2], where gauge invariance is maintained via a Higgs mechanism). As far as the quarks are concerned, we simply assume that confinement affects the gluons at shorter distances than it affects the quarks. This does not break the gauge invariance of the

$O(\alpha_s^2)$ calculation, as the gluon propagator does not enter the quark-gluon WST identities. Recent results on the quark propagator in the axial gauge confirm that a simple pole in the quark propagator is not far from the true solution [17].

Hence the replacement of the gluon propagator by a nonperturbative counterpart does not violate gauge invariance for gluon exchange diagrams. One can think of this replacement as the inclusion of a subclass of diagrams (the gluon self-energy) which are resummed via nonperturbative methods (the DS equations). Although these diagrams are supposedly sub-leading $\log s$, their inclusion certainly changes the leading-log answer.

The contributions to proton-proton scattering at $t = 0$ are of two kinds: the $\mathcal{E}_1^2$ term of formula (2.10) leads naturally to the quark counting rule and to an effective pomeron vertex behaving like γ^μ [7, 18]. This is due to the fact that along two quark lines of momentum p_1 and p_2 we can write $[\gamma_\mu(p_1.\gamma)\gamma_\nu] \otimes [\gamma^\mu(p_2.\gamma)\gamma^\nu] \approx 2s\gamma_\mu \otimes \gamma^\mu$. On the other hand, the terms containing $\mathcal{E}_2$ do not have such a simple structure, as they involve the hadronic wavefunction in the middle of the preceeding expressions.

However, this hadronic wavefunction must contain a scale, the hadronic radius R. If gluons propagate only to finite distances, *i.e.* if the gluon propagator is smoothed in the infrared region, then one can produce a damping of the $\mathcal{E}_2$ terms. A simple dimensional argument leads to the conclusion that a damping in the infrared region means the introduction of a nonperturbative scale μ_0, such that the gluon propagator now looks like:

$$D(q^2) = \frac{1}{\mu_0^2}\,\mathcal{D}(\frac{q^2}{\mu_0^2}) \tag{2.21}$$

with $\mathcal{D}$ a function without a pole at the origin. In the case $\mu_0 >> 1/R$, the propagator hardly changes while the form factor drops sharply, so that one gets a suppression factor $(\mu_0 R)^{-2}$. This suppression of the $\mathcal{E}_2$ terms in turn leads to a better agreement of the elastic differential cross section with experiment, as it is already known that a $\gamma^\mu \otimes \gamma_\mu$ combined with the parametrization (2.15) leads to a good fit to the data [1].

The problem remains however to see whether such a simple idea can be theoretically justified. One indeed expects gluons not to propagate to infinity: their self-interaction should confine them, and thus modify their propagator. Lattice studies suggest that the gluon propagator is suppressed at small momentum transfer [19], but its exact structure remains unclear. By studying the Dyson-Schwinger equation for the gluon propagator [8, 9] or the Gribov horizon [20], several groups have recently confirmed that such a picture is essentially correct. the Dyson-Schwinger equations have been shown to possess, in their truncated form, at least two types of solutions: those that behave like $1/k^4$ at the origin,

as well as smoother ones. As the $1/k^4$ solutions do not have a Hilbert transform, we do not know how to use them in diffractive calculations. We thus assume that the other solutions, which do not have poles for $q^2 \leq 0$, are those which are relevant for diffractive scattering. These solutions have been derived in various gauges. In the following, we shall consider only gauge-invariant sets of diagrams, so that the dependence on the propagators comes from the different approximations made by the authors of references [8, 9].

Although the asymptotic forms of [8, 9] agree with perturbative QCD at large k^2, there is a wide disagreement as to the details of their behaviour near $k^2 = 0$: they either go to zero [9, 20], or are finite [10], or are infinite [8]. We limit ourselves here to the study of three propagators which represent the whole range of behaviours at the origin which can be implemented in the calculation (assuming that the propagator does not change sign for $q^2 < 0$.) Note that we have considered several other possibilities (massive propagators, exponential propagators, perturbative propagator with a cutoff) with similar results [21].

The Häbel-Könnig-Reusch-Stingl-Wigard (HKRSW) propagator [9] vanishes at the origin. Its form has been suggested by a consistency argument in the Landau gauge, and agrees with that derived by Zwanziger based on considerations related to the Gribov horizon [20].

$$D(k^2) = \frac{1}{k^2 + \mu_0^4/k^2} \tag{2.22}$$

In the axial gauge, Cornwall has derived a gauge-invariant set of diagrams defining a gluon mass [10]. Although one might worry about simply putting this mass into an explicitly gauge dependent object, it enables us to consider the possibility of a propagator finite at the origin:

$$\alpha_s D(k^2) = \left\{ \frac{27}{12\pi} \left(k^2 + \mu^2(k^2)\right) \log \left(\frac{(k^2 + \mu^2(k^2))}{\Lambda^2_{QCD}} \right) \right\}^{-1} \tag{2.23}$$

where:

$$\mu^2(k^2) = \mu_0^2 \left(\frac{\log(4\mu_0^2/\Lambda^2_{QCD})}{\log((k^2 + 4\mu_0^2)/\Lambda^2_{QCD})} \right)^{12/11} \tag{2.24}$$

Notice that in the axial gauge, a theorem due to Baker, Ball and Zachariasen implies that the gauge-dependent propagator is infinite at the origin [22]. Solutions have been found by D.A. Ross and one of us [8] which behave like a fractional power of k^2 near $k^2 = 0$:

$$D(k^2) = \frac{1}{\mu_0^2 \left(0.88 \left(\frac{k^2}{\mu_0^2}\right)^{0.22} - 0.95 \left(\frac{k^2}{\mu_0^2}\right)^{0.86} + 0.59 \left(\frac{k^2}{\mu_0^2}\right) \log \left(2.1 \left(\frac{k^2}{\mu_0^2}\right) + 4.1 \right) \right)} \tag{2.25}$$

As far as the treatment of α_s goes, propagator (2.23) uses a running coupling, which is included in its expression. (We use a value $\Lambda_{QCD} = 0.3$ GeV, as in the perturbative case.) The HKRSW propagator is at fixed coupling, and renormalization group effects have not been included. The axial gauge propagator (2.25) does include renormalization group effects. The corresponding α_s is fixed and of the order of 1 [8]. Hence, for propagators (2.22, 2.25) we shall use a fixed $\alpha_s = 1$ and indicate how our results scale with α_s.

2.4. Phenomenology of two-gluon exchange

Each of the above propagators contains an intrinsic scale μ_0: as QCD is a scale-free theory, this scale cannot be determined directly from Dyson-Schwinger equations, and must thus be determined through comparison with some dimensionful quantity. We shall assume from now on that two-gluon exchange gives the bulk of the cross sections, and that higher orders contribute to the s-dependence of the result. More precisely, as the total cross sections are well fitted to 22 mb s^{ϵ_0} [1], we assume that the lowest order must give us a number of the order of 22 mb. The logarithmic slope at the origin is a constant of the order of 10 GeV^{-2} plus terms that behave like $\log s$. Again, we assume that two-gluon exchange will give us the constant piece. As the quark-counting rule is essentially independent of energy (at least in the region where we have data), we assume it must be obeyed too. These are thus the three tests to which we want to submit the above propagators. Note that it is not entirely obvious that all three can be passed, as we have three quantities and one parameter.

We show in Figure 6 the dependence of σ_{tot}^{pp} (a), B(0) (b) and $\sigma_{tot}^{\pi p}/\sigma_{tot}^{pp}$ (c) on the scale μ_0 entering the propagator. As a growing μ_0 makes the propagator smaller, it is not surprising that the total cross section goes down with the propagator scale, as shown in Figure 6(a). It is less obvious however that for $\mu_0 \sim 0.3 - 1.0$ GeV, one gets a large suppression factor, and thus each propagator can give a good starting value for the total cross section, of the order of 20 mb. The logarithmic slope of the elastic cross section also gets cured by the introduction of μ_0, and numbers of the order of 10 GeV^{-2} can be achieved for scales of the same order. Note in passing that if we were to take these results at face value, propagator (2.23) would have to be disfavoured as it cannot simultaneously reproduce $B(0)$ and σ_{tot}. However, the two-gluon exchange process is certainly a very rough approximation, hence fitting results to this order is certainly misleading.

If we now turn to Figure 6(c), we see that the quark counting rule, which can be accounted for by the perturbative calculation, is now slightly modified by nonperturbative

effects. For moderate values of μ_0, we get a result which is smaller than the perturbative one, and thus in better agreement with the data. For large μ_0, the ratio goes to 2/3 as the $\mathcal{E}_2$ terms are more and more suppressed. Figure 6(d) shows the ratio of the terms for which $\mathcal{E}_2$ contributes to those which depend only on $\mathcal{E}_1^2$ in formula (2.10). We see that the Landshoff-Nachtmann suppression is present to some extent for all propagators, but that only propagator (2.22) gives a suppression which ensures the factorizability of the pomeron coupling.

We thus see at this order that nonperturbative effects are non-negligible. The inclusion of modified propagators in the calculation provides appreciable improvements, and the improved order α_s^2 constitutes a good starting point for an expansion in $\log s$. Let us now see to which extent these improvements carry over to higher orders.

3. Gluon exchange to order α_s^3

3.1. General formalism for three-gluon exchange

The lowest-order QCD diagrams contributing to $C = -1$ exchange between quarks are those of Figure 7. By contour integration, we obtain the following for the amplitudes, before the inclusion of the colour algebra:

$$\begin{aligned} \mathcal{A}_{(a)} &= \mathcal{A}_{(b)} = -64\pi\alpha_s^3 s \log s \; [I_R] \\ \mathcal{A}_{(c)} &= \mathcal{A}_{(d)} = 32\pi\alpha_s^3 s \log s \; [I_R - i\,\pi\, I_i] \\ \mathcal{A}_{(e)} &= \mathcal{A}_{(f)} = 32\pi\alpha_s^3 s \log s \; [I_R + i\,\pi\, I_i] \end{aligned} \tag{3.1}$$

with

$$I_i = \int [\prod_{j=a,c} \frac{d\vec{k}_j}{(2\pi)^2}] \frac{(2\pi)^2\,\delta^{(2)}\left(\sum_{j=a,c} \vec{k}_j - \vec{\Delta}\right)}{\prod_{j=a,c}\left(\vec{k}_j^{\,2} + \sigma_j\right)} \tag{3.2}$$

I_R is a rather complicated function of the momenta, but, as we are about to explain, we shall not need it in the following.

The colour algebra involves terms like $Tr(\lambda_a\lambda_b\lambda_c)Tr(\lambda_{a'}\lambda_{b'}\lambda_{c'})$ with a', b', c' some combination of a, b, c. Using the fact that $Tr(\lambda_a\lambda_b\lambda_c) = 2(if_{abc} + d_{abc})$, we recognize that the amplitude will contain two terms, one proportional to $f_{abc}f_{abc}$ and one proportional to $d_{abc}d_{abc}$. When we calculate $\bar{q}q$ scattering instead of qq, the first term flips sign while

the second remains the same. As antiquarks and quarks couple to gluons with opposite signs, the first term will contribute to the pomeron, while the second will give the lowest-order odderon. As the pion has the same number of quarks and antiquarks, the odderon contribution vanishes, whereas for the proton one obtains a nonzero contribution.

3.2. The commuting (odderon) case

As Eq. (3.1) shows, when we add all the diagrams of Figure 7 we obtain zero. This means that there are no leading-log contributions to the odderon at this order. As d_{abc} is a commuting object, we can apply the QED formalism developed in Ref. [18]. For quark-quark scattering, one easily obtains the third-order result:

$$\mathcal{A}_O = \frac{(4\pi)^3 \alpha_s^3}{3} s \int [\prod_{j=a,c} \frac{d\vec{k}_j}{(2\pi)^2}] \frac{(2\pi)^2 \delta^{(2)}\left(\sum_{j=a,c} \vec{k}_j - \vec{\Delta}\right)}{\prod_{j=a,c} \left(\vec{k}_j^{\,2} + \sigma_j\right)} \tag{3.3}$$

for the sum of the diagrams of Figure 7. The quark propagators transform into θ-functions ordering the vertices in x^+ and x^- space. These theta functions in turn combine together, and one is left with a δ function, which makes the p^+ and p^- integrations trivial: at every stage, the quarks remain on the light-cone.

This means that formula (2.8) can be applied directly. Expanding it to order α_s^3, and carrying out the required colour traces, we obtain no odderon contribution in $p\pi$ scattering whereas pp scattering gives:

$$\begin{aligned}
\mathcal{A}_O &= -\frac{10}{9\pi}\alpha_s^3 s \int d\vec{k}_a d\vec{k}_b d\vec{k}_c \\
&\times \frac{1}{\vec{k}_a^{\,2} + \sigma_a} \frac{1}{\vec{k}_b^{\,2} + \sigma_b} \frac{1}{\vec{k}_c^{\,2} + \sigma_c} \delta^{(2)}(\vec{k}_a + \vec{k}_b + \vec{k}_c - \vec{\Delta}) \\
&\times [\mathcal{E}_1(\vec{k}_a + \vec{k}_b + \vec{k}_c) + 2\,\mathcal{E}_3(\vec{k}_a, \vec{k}_b, \vec{k}_c) \\
&- \mathcal{E}_2(\vec{k}_a + \vec{k}_b, \vec{k}_c) - \mathcal{E}_2(\vec{k}_b + \vec{k}_c, \vec{k}_a) - \mathcal{E}_2(\vec{k}_c + \vec{k}_a, \vec{k}_b)]^2
\end{aligned} \tag{3.4}$$

with $\mathcal{E}_1$ and $\mathcal{E}_2$ the two form factors encountered previously (2.11, 2.12), and

$$\mathcal{E}_3(\vec{k}_a, \vec{k}_b, \vec{k}_c) = \int d\mathcal{M}\; e^{i\vec{k}_a \cdot \vec{r}_k + i\vec{k}_b \cdot \vec{r}_l + i\vec{k}_c \cdot \vec{r}_m} \tag{3.5}$$

with $k \neq l \neq m$.

The third form factor $\mathcal{E}_3$ corresponds to diagrams where one gluon gets attached to each quark. As was the case for two-gluon exchange, formula (3.4) is infrared convergent. This is due to the fact that $\mathcal{E}_3$ reduces to $\mathcal{E}_2$ when one of its momenta vanishes:

$$\mathcal{E}_3(0, \vec{k}_b, \vec{k}_c) = \mathcal{E}_2(\vec{k}_b, \vec{k}_c) \tag{3.6}$$

and similar conditions when $\vec{k}_b \to 0$, $\vec{k}_c \to 0$.

We shall use only a simple parametrization of $\mathcal{E}_3$ in this case, based on the previous one for $\mathcal{E}_2$ (2.17):

$$\mathcal{E}_3(\vec{k}_a, \vec{k}_b, \vec{k}_c) = \mathcal{E}_1 \left(\vec{k}_a^2 + \vec{k}_b^2 + \vec{k}_c^2 - f(\vec{k}_a.\vec{k}_b + \vec{k}_a.\vec{k}_c + \vec{k}_b.\vec{k}_c) \right) \tag{3.7}$$

This form gives rise to the expression (2.17) via the use of Eq. (3.6). We can now see why $f = 1$ is the solution for the proton which corresponds to $f = 2$ in the pion case: when the three quarks are scattered by the same amount in transverse space, if they have the same longitudinal momentum, they must recombine into a proton. This is the same argument as for formula (2.18) in the pion case. Thus

$$\mathcal{E}_3(\vec{k}, \vec{k}, \vec{k}) = 1 \tag{3.8}$$

This implies that we have $f = 1$ in the proton case, and also the form (2.17) for $\mathcal{E}_2$.

As already pointed out [5], the $\mathcal{E}_3^2$ term of Eq. (3.4) will dominate the elastic amplitude at high-t. We can see this from formula (3.8): configurations for which the three quarks are scattered by the same amount will not be affected by the sharp t-dependence coming from $\mathcal{E}_1$ or $\mathcal{E}_2$.

Note however that in this formalism, the exact high-$|t|$ behaviour of the elastic amplitude depends on the details of the wavefunction. The terms proportional to $\mathcal{E}_1^2$ will naturally reproduce the dimensional counting rule at high t (at least once an infrared regulation makes them finite). However, for $\mathcal{E}_2$ and $\mathcal{E}_3$ can accommodate a wide range of t-dependences: looking at formulae (2.17, 3.7), we see that depending on the value of f, we can get behaviours similar to F_1 for $f = -2$, or totally flat for $f = 1$ (2) in the proton (resp. pion) case. Furthermore, the simple guesses (2.17, 3.7) were motivated by an infrared argument, which certainly does not account for the process of reference [5]. Similarly, the only test for the wavefunction (2.19) has been the reproduction of the Dirac form factor F_1. Hence it is not surprising that a reproduction of the Landshoff mechanism will necessitate a closer study of the wavefunction to pin down the t-dependence of these terms. We shall simply

mention here that the t^{-8} behaviour *can* be implemented in our calculation, but it relies on a fine-tuning of the hadronic wave function.

On the other hand, notice that $\mathcal{E}_3$ is present (at this order) only for $C = -1$ contributions. Although the odderon is dominant at high-t, it is suppressed at small t, because of the structure of its form factor $\mathcal{E}_1 - 3\mathcal{E}_2 + 2\mathcal{E}_3$. As can be seen from Table 2, in pertubative QCD the odderon contribution to the amplitude at $t = 0$ is about 18% of the two-gluon exchange amplitude.

Thus at this order, the amplitude is purely real, and contains three form factors. These are the only three possible form factors that will occur at any order in pp scattering. We notice that the amplitude takes a form that involves only propagators, so that we are allowed to replace $1/(\vec{k}^2 + \sigma)$ by a nonperturbative estimate $D(k^2)$ in Eq. (3.4), using formula (2.20).

3.3. The anticommuting (pomeron) case

One has to be a little more careful when one evaluates the contributions of the diagrams of Figure 7 to the pomeron. As we have seen, these $C = +1$ contributions will come from the anticommuting part of the colour algebra, and thus will flip the sign of some of the expressions of Eq. (3.1). This means that the leading-log contributions will not cancel anymore, and thus we shall have a $\log s$ contribution. A naïve application of formula (2.8), taking ordering in the x^+ and x^- directions leads to the counterpart of Eq. (3.4):

$$\begin{aligned} \mathcal{A}_{\mathcal{P}} &= \frac{4}{3\pi^2} n_1 n_2 \alpha_s^3 is \log s \int d\vec{k}_a d\vec{k}_b d\vec{k}_c \\ &\times \frac{1}{\vec{k}_a^{\,2} + \sigma_a} \frac{1}{\vec{k}_b^{\,2} + \sigma_b} \frac{1}{\vec{k}_c^{\,2} + \sigma_c} \delta^{(2)}(\vec{k}_a + \vec{k}_b + \vec{k}_c - \vec{\Delta}) \\ &\times \mathcal{F}_{\mathcal{P}}(\vec{k}_a, \vec{k}_b, \vec{k}_c) \end{aligned} \tag{3.9}$$

with

$$\begin{aligned} \mathcal{F}_{\mathcal{P}}(\vec{k}_a, \vec{k}_b, \vec{k}_c) &= \frac{1}{2}[\mathcal{E}_1^{h_1}(\vec{k}_a + \vec{k}_b + \vec{k}_c) - \mathcal{E}_2^{h_1}(\vec{k}_a + \vec{k}_b, \vec{k}_b)] \\ &\times [\mathcal{E}_1^{h_2}(\vec{k}_a + \vec{k}_b + \vec{k}_c) - \mathcal{E}_2^{h_2}(\vec{k}_a + \vec{k}_b, \vec{k}_c) \\ &\quad -\mathcal{E}_2^{h_2}(\vec{k}_b + \vec{k}_c, \vec{k}_a) + \mathcal{E}_2^{h_2}(\vec{k}_c + \vec{k}_a, \vec{k}_b)] \\ &\quad +\{h_1 \leftrightarrow h_2\} \end{aligned} \tag{3.10}$$

It is interesting that once again, the expressions (3.1) will combine to allow the use of

nonperturbative propagators, via the integration of the $1/(\vec{k}^2+\sigma)$ with a Källen-Lehmann density, as explained in the two-gluon case (2.20).

The log s comes from large rapidity gaps, *i.e.* one of the gluons will have to carry both a large + and a large − components (by "large" we mean bigger than $O(1/s)$). But one must then be very careful that the final state does not develop a large mass of the order of $\sqrt{s}$: if a line going in the + direction with momentum $\sqrt{s}$ absorbs a momentum k_- going in the − direction, it will develop a mass $\sqrt{s}k_- >> m_h$, and thus will be able to combine with the other quarks only after another gluon has carried that k_- component. For example, we show in Figure 8 a configuration which is always suppressed.

The effect of these large masses will be to destroy some of the contributions to formula (3.9). In order to decide which terms get suppressed, we use the fact that hadron-hadron scattering has the same structure as photon-photon scattering. Hence, although in the hadronic case the use of cutting rules is obscured by the fact that some of the propagators are absorbed in the wavefunction, as illustrated by Eq. (2.6), the argument of Ref. [2] can be applied to the hadronic case. In both cases, the propagators that generate a large final-state mass are suppressed, so that the remaining form factors are the same as those derived in the eikonal approximation. Rederiving the results of reference [2], we obtain, instead of (3.10) in Eq. (3.9):

$$\begin{aligned}\mathcal{F}_{\mathcal{P}}(\vec{k}_a,\vec{k}_b,\vec{k}_c) &= \frac{1}{2}\mathcal{F}_1^{h_1}\mathcal{F}_1^{h_2}-\frac{1}{4}(\mathcal{G}_a^{h_1}\mathcal{G}_a^{h_2}+\mathcal{G}_c^{h_1}\mathcal{G}_c^{h_2})\\ &+ \mathcal{F}_1^{h_1}(\mathcal{G}_a^{h_2}+\mathcal{G}_c^{h_2})+\mathcal{G}_a^{h_1}\mathcal{G}_c^{h_2}\\ &\quad +(h_1\leftrightarrow h_2)\end{aligned}$$

where $\mathcal{F}_1=\mathcal{E}_1(\vec{k}_a+\vec{k}_b+\vec{k}_c)$, $\mathcal{G}_a=\mathcal{E}_2(\vec{k}_a,\vec{k}_b+\vec{k}_c)$ and $\mathcal{G}_c=\mathcal{E}_2(\vec{k}_c,\vec{k}_a+\vec{k}_b)$.

3.4. The complete pomeron to order α_s^3

In order to compute the full order α_s^3 contributions to the pomeron, we need to add the H and Y diagrams of Figure 9. As is well known [18], when the gluons are exchanged between two quark lines, these diagrams mostly cancel, and give a contribution proportional to $\mathcal{E}_1^2$. It turns out that this almost exact cancellation holds also for the diagrams where different quarks within the same hadron contribute. That is because the Y diagram contributes in the configuration of Figure 10(a), which reproduces exactly the form factor of Figure 10(b): each line is hit by the same amount.

Although the Soper-Gunion formalism does not explicitly include these, it is not very hard to convince oneself that the form factors will be the same as in two-gluon exchange, so that we get for the sum of the diagrams of Figure 7:

$$\begin{aligned} & -\frac{4}{3\pi^2}\vec{\Delta}^{\,2} n_1 n_2 \alpha_s^3 i s \log s \int d\vec{k}_a d\vec{k}_b \\ & \times \frac{\left(\mathcal{E}_1^{h_1}(\vec{\Delta}) - \mathcal{E}_2^{h_1}(\vec{\Delta}-\vec{k}_a,\vec{k}_a)\right)\left(\mathcal{E}_1^{h_2}(\vec{\Delta}) - \mathcal{E}_2^{h_2}(\vec{\Delta}-\vec{k}_b,\vec{k}_b)\right)}{(\vec{k}_a^{\,2}+\sigma)\left((\vec{\Delta}-\vec{k}_a)^{\,2}+\sigma\right)(\vec{k}_b^{\,2}+\sigma)\left((\vec{\Delta}-\vec{k}_b)^{\,2}+\sigma\right)} \end{aligned} \tag{3.11}$$

with $\mathcal{E}_1$ and $\mathcal{E}_2$ the form factors introduced in formulae (2.11,2.12). Notice that, once more, assuming the existence of a Källen-Lehmann density for the gluon propagator enables us to change $1/(\vec{k}^2+\sigma)$ into $D(k^2)$.

4. Phenomenology of the order α_s^3 results

4.1. General structure of the answer

As we have shown in the previous sections, the complete order α_s^3 formalism leads to a hadronic amplitude that has the following form:

$$\mathcal{A}(s,t) = \mathcal{A}_2\left\{i\left[1+\log s\left(\epsilon_0+\alpha' t+O(t^2)\right)\right]+f_{odd}(t)\right\} \tag{4.1}$$

It is of course tempting to see in this a first-order Taylor expansion in $\log s$ of a pomeron pole, plus a zeroth-order term from an odderon pole. There would then be a one-to-one mapping between the Regge picture of the pomeron and this calculation. As BFKL have shown [2], life is not so simple, and higher-order terms spoil the analogy. Hence in the following the terms "pomeron intercept" or "slope" must not be taken literally. As we shall now see, all the problems of the BFKL formalism [6] are already present at this low order. It is thus worth examining them in the context of the simple equations we have gathered in this paper, rather than obscuring the issues by resumming.

At this order, the normalization of the cross section, $\mathcal{A}_2$, comes from two-gluon exchange, formula (2.10). The pomeron intercept, $1+\epsilon_0$, is the ratio of two to three gluon exchange, formula (2.10, 3.9). The odderon contribution f_{odd} comes of course from Eq. (3.4). Finally, the α' contribution will come from Eq. (3.11) and from the Taylor expansion of Eq. (3.9).

The perturbative results are shown in Table 2. As we have mentioned earlier, the modifications to the gluon propagator that we shall discuss in the following will diminish

the dependence of the results on the choice of form factors. Therefore, the 25% variations that we get in ϵ_0 and σ_2 can be considered as upper bounds on the theoretical uncertainty from form factors. For simplicity, we shall only consider the parametrization (2.15, 2.17, 3.7) in the following.

The interest of running α_s becomes obvious at third order. The main problem here is that ϵ_0 is much too large. Running the coupling will reduce the effect of the third gluon, and thus lower ϵ_0. As Table 2 shows, it does not decrease it enough. The running α_s that we used can in fact be mimicked by a fixed $\alpha_s = 0.72$. Similarly, the odderon contribution is in turn further suppressed by the running, to about 8% of the 2-gluon exchange amplitude.

Another obvious problem is the fact that, although the expression (3.11) is finite for $\vec{\Delta} \to 0$, it does not lead to a finite value for α': the integrands at $\vec{\Delta} = 0$ look like $(\mathcal{E}_1 - \mathcal{E}_2)/k^4$, and we thus have a logarithmically divergent α'.

Finally, we show that at this order the pomeron does not appear to be a universal object: we calculated J/ψ p scattering, using a monopole form factor for the J/ψ similar to Eq. (2.16) but with $\sqrt{< r^2_{J/\psi} >} = 0.2$ fm [16]. We then obtain a 15% difference in the coefficient of the log s term.

4.2. Nonperturbative effects

As we have already mentioned, we can easily accommodate nonperturbative propagators in the expression given for the hadronic amplitude. Provided that the propagators have the usual analytic properties embodied by the Källen-Lehmann density, the prescription is simply to replace $1/(k^2+\sigma)$ by the nonperturbative prescription for the propagator, $D(k^2)$. Note that the reason why such a simple prescription works remains obscure, as in principle a more complicated structure for the hadronic amplitude is allowed. In fact, were the real part I_R of Eq. (3.2) not to cancel, the situation would be more complicated as the integral over σ would not simply reproduce the gluon propagators. It happens, at least at this order of perturbation theory, that the amplitude effectively involves only t-channel propagators. Before describing the effect of propagators (2.22, 2.24, 2.25) on the amplitude, we wish to point out that a simple bound will apply at this order, provided the propagator does not flip sign.

The form factor in the odderon part of the amplitude (3.4) provides a more effective suppression than the form factor entering the pomeron contribution (3.9). One therefore

obtains:

$$f_{odd} \leq \frac{54}{5\pi}\epsilon_0 \tag{4.2}$$

If some mechanism can bring ϵ_0 to be in agreement with data, and hence be of the order of 0.1, we expect the lowest-order odderon to be similarly modified, and hence relation (4.2) to be still true.

Figure 11 shows in details the result of the use of propagators (2.24, 2.22, 2.25), as a function of the nonperturbative scale μ_0. Figure 11(a) shows that ϵ_0 can in principle get as low as 0.35. For values of μ_0 favoured by our previous discussion on two-gluon exchange, we see that we get values of the order of 2 for the intercept: it thus seems impossible to get acceptable numbers both for two and three-gluon exchange. Another way to look at this is to allow α_s to vary: for values around 0.1, one would indeed get an intercept compatible with data, but that would mean that although rising at the correct rate, the pomeron cross section would be much too low.

Figure 11(b) shows that the pomeron slope becomes finite once the infrared region is smoothed out. Values compatible with 0.25 GeV can again be achieved, but again for values of μ_0 or α_s that would suppress two-gluon exchange.

Figure 11(c) shows the pomeron trajectories that we obtain for the values of μ_0 giving 22 mb for the total two-gluon cross section, *i.e.* 0.282 GeV for (2.24), 0.491 GeV for (2.22) and 0.946 GeV for (2.25). The trajectories are much flatter than in the perturbative case, and that their slopes are finite.

Finally, we show in Figure 11(d) that the ratio of the odderon amplitude to the two-gluon exchange one tends to be greater or equal to the perturbative answer. This simply means that it falls more slowly with increasing μ_0 than two-gluon exchange. Similarly, $\epsilon_0(J/\psi\ p)$ is again roughly 10 to 15% larger than $\epsilon_0(pp)$.

Hence there is no "golden propagator". The three propagators we have tried have met with some success, but none of the gives us a perfect fit. None of them can accommodate a sizeable two-gluon exchange amplitude together with a slowly rising third-order amplitude. At third order, propagator (2.24) gives the most promising results. One has to point out however that this is mainly due to the fact that the α_s used is appreciably smaller than in the case of the two other propagators.

5. Conclusion

We have shown in this paper that the Soper-Gunion formalism can be extended to include three-gluon effects, and that the proton possesses three form factors, in the valence quark approximation. The structure of these form factors naturally suppresses the odderon at small t and makes it leading at high-t.

The preceeding study has also shown that the infrared region is important in leading $\log s$ calculations. Although the perturbative answer is infrared finite, the dominant region of k^2 remains small until t is as large as 10 GeV. We have shown that nonperturbative effects can change the answer by large factors, of the order of 3. Before meaningful comparisons can be made with deep inelastic experiments, or with diffractive ones, one will have to understand this region better.

The use of recent solutions to the Dyson-Schwinger equation, combined with the simple idea that it is enough to modify the gluon propagator at small momentum transfer [7], is not sufficient to diminish the value of the pomeron intercept to bring it in agreement with data.

It is surely possible to find a functional form for the gluon propagator that will bring the result in closer agreement with experiment. This can in principle be repeated order by order. Given the wide variety of behaviours at the origin which we have examined in this paper, the functional form of the propagator should have one of the following forms: either be suppressed near the origin faster that propagator (2.22), or change sign in the t-channel. It is however unlikely that such a phenomenological procedure would lead to a propagator exhibiting the correct properties at high k^2.

One could of course criticize the use of a loop expansion in a region which is *a priori* nonperturbative. However, it is interesting to notice that the perturbative calculation gives an answer which is qualitatively correct. Hence the idea of a loop expansion, or even the concept of quarks and gluons seem to be fruitful in this context.

Another possibility is that at these high values of α_s, the loop expansion exhibits its asymptotic character very early, and that the lowest-order term is as far as we will ever get. The use of nonperturbative propagators in the lowest-order expression has already led to a qualitatively successful phenomenology [7, 16, 17, 23]. It could be that the third order already departs from the true answer.

Before jumping to such drastic conclusions, one has to re-examine the procedure used

to derive the results of this paper.

First of all, we are using a leading-log s procedure. For this to make sense, the sub-leading terms from the third order must be smaller than the second order. We can get a rough estimate of the size of these terms: s to u crossing symmetry of the amplitude implies that $\log s$ must be replaced by $(\log(s) + \log(-s))/2 = \log s - i\pi/2$. Hence the ratio of the sub-leading terms to the leading ones of the previous order should be about $i\pi\epsilon_0/2$. For the magnitude of this to be small, we certainly need $\epsilon_0 << 2/\pi$. Therefore, unless the intercept ϵ_0 is small, the leading-log s calculation probably does not make sense. For the perturbative calculation, demanding that sub-leading terms are half of the leading ones at the preceeding order leads to: $\alpha_s < 0.15$. As we are trying to reduce the value of the intercept, this would at the same time lower the sub-leading terms and put the leading-log s approximation on firmer ground.

Two basic ingredients need to be implemented before one can present final conclusions. First of all, the simple replacement of the gluon propagator by a solution of the Dyson-Schwinger equation explicitly breaks gauge invariance in the H and Y diagram of Figure 10. Explicit solutions for the vertices are known [22], and such a procedure would definitely modify our estimate of α'.

Furthermore, the fact that the three-gluon exchange diagrams of Figure 6 involve only gluon propagators in the t-channel remains puzzling, as the answer can be obtained by cutting rules, and as some of the cuts involve the gluons. There must thus be a precise interplay between the gluon and quark propagators for this property to be conserved. A re-examination of the cutting rules in the context of modified propagators seems needed. Indeed, for three-gluon exchange, the cuts through quark lines contribute precisely $-1/2$ of the cuts though gluon lines. Were the cutting rules to be modified by nonperturbative effects, this delicate balance could be broken and the result turn out to be entirely different. We plan to address these questions in the future.

Acknowledgements

We wish to acknowledge discussions with P.V. Landshoff, L.N. Lipatov, B. Margolis and D. Soper. This work was supported in part by NSERC (Canada) and les fonds FCAR (Québec).

quantity	fixed α_s	running α_s
$\sigma_2(pp)/\alpha_s^2$	75.8 (59.6) mb	63.5 (46.6) mb
$B(0)$	∞	∞
$\sigma_2(p\pi)/\sigma_2(pp)$	0.654	0.660

Table 1: the perturbative results at order α_s^2

quantity	fixed α_s	running α_s
$\alpha_0(pp)/\alpha_s$	1.87 (1.82)	1.36 (1.20)
$\alpha_0(p\pi)/\alpha_s$	1.75	1.25
$\sigma_{odd}/\alpha_s\sigma_2$	0.174	0.079
α'	∞	∞
$\alpha_0(J/\psi p)/\alpha_0(pp)$	1.15	1.23

Table 2: the perturbative results at order α_s^3

FIGURE CAPTIONS

Figure 1: Two-gluon exchange contributions to quark-quark scattering. The dashed lines represent gluons and the plain ones represent quarks.

Figure 2: Two-gluon exchange contributions to photon-photon scattering. (a) gives rise to the $\mathcal{E}_1(\vec{k}_a + \vec{k}_b)$ and (b) to $\mathcal{E}_2(\vec{k}_a, \vec{k}_b)$.

Figure 3: The Dirac form factor $\mathcal{E}_1$ from formula (2.12) (dashed curve), compared with the form resulting from a dipole parametrization of G_E [14] (plain curve).

Figure 4: The elastic differential cross section at $O(\alpha_s^4)$, as predicted by perturbative QCD. The plain curve is for fixed $\alpha_s = 1$ and scales like α_s^2, the dashed one for a running α_s (see text).

Figure 5: The average gluon momentum flowing through the perturbative two-gluon exchange graphs for fixed α_s (plain curve) and running α_s (dot-dashed curve).

Figure 6: Two-gluon exchange results for three nonperturbative gluon propagators, Cornwall (plain curve), Eq. (2.24), Häbel-Könnig-Reusch-Stingl-Wigard (dashed curve), Eq. (2.22) and Cudell-Ross (dot-dashed curve), Eq. (2.25). The horizontal axis gives the nonperturbative scale entering the propagator. (a) shows the total proton-proton cross section, which scales like α_s^2, (b) gives the logarithmic slope at $t = 0$ of the elastic cross section, (c) the ratio of the pion-proton to the proton-proton cross sections and (d) the ratio of the terms in the amplitude where gluons hit only one quark line to those where gluons hit two quark lines.

Figure 7: Three-gluon exchange contributions to hadron-hadron scattering. We show the diagrams proportional to $\mathcal{E}_1(\vec{k}_a + \vec{k}_b + \vec{k}_c)^2$.

Figure 8: One of the diagrams that always gets suppressed because the final state develops a large mass.

Figure 9: Some of the H, X and Y diagrams contributing to the pomeron slope.

Figure 10: Both diagrams give rise to the same form factor $\mathcal{E}_2(\vec{k}_a, \vec{\Delta} - \vec{k}_a)\ \mathcal{E}_1(\vec{\Delta})$.

Figure 11: Order α_s^3 results for the three nonperturbative gluon propagators of Figure 6. Our convention for the curves is the same as in Figure 6. μ_0 is the nonperturbative scale entering the propagator. All graphs scale like α_s. (a) shows the ratio at $t = 0$ of the coefficient of the $\log s$ term to the two-gluon exchange term; (b) the ratio at $t = 0$ of

the coefficient of the $t \log s$ term to the two-gluon exchange term; (c) shows the pomeron trajectory at this order for the values of μ_0 which give 22 mb for the two-gluon exchange cross section, the thick curve is the trajectory in the perturbative answer; (d) gives the ratio of the third order odderon amplitude to the imaginary part of the two-gluon amplitude.

References

[1] A. Donnachie and P.V. Landshoff, Nucl. Phys. **B244** (1984) 322; **B267** (1985) 690; Phys. Lett. **B296** (1992) 227

[2] V.S. Fadin, E.A. Kuraev and L.N. Lipatov, Phys. Lett. **60B**; Y.Y. Balitskiĭand L.N. Lipatov, Sov. J. Phys. **28** (1978) 822

[3] K. Goulianos, Physics Reports **101** (1983) 169

[4] D.G. Richards, Nucl.Phys. **B258** (1985) 267

[5] A. Donnachie and P.V. Landshoff, Phys. Lett. **123B** (1983) 345, P.V. Landshoff, Phys. Rev. **D 1024** (1974) 1024

[6] R.E. Hancock and D.A. Ross, Nucl.Phys. **B394** (1993) 200 and **B383** (1992) 575

[7] P.V. Landshoff and O. Nachtmann, Z. Phys. **C35** (1987) 405

[8] J. R. Cudell and D.A. Ross, Nucl. Phys. **B359** (1991) 247
J.R. Cudell, Proceedings of the 4^{th} Blois Workshop on Elastic & Diffractive Scattering, La Biodola, Italy (1991).

[9] U. Häbel, R. Könning, H.G. Reusch, M. Stingl and S. Wigard, preprint Print-89-0128 (MUNSTER) and Z. Phys. **A336** (1990) 435

[10] J.M. Cornwall, Phys.Rev. **D26** (1982) 1453

[11] F.E. Low, Phys. Rev. **D12** (1975) 163; S. Nussinov, Phys. Rev. Lett. **34** (1976) 1286

[12] H. Cheng and T.T. Wu, Phys. Rev. Lett. **24** (1970) 1456
V.N.Gribov, L.N. Lipatov and G.V. Frolov, Sov. J. Nucl. Phys. **12** (1971) 543

[13] J.F. Gunion and D. Soper, Phys. Rev. **D 15** (1977) 2617

[14] P.N. Kirk et al., Phys. Rev. **D8** (1973) 63
R.H. Hodstadter, F. Bumiller and M.R. Yearian, Rev. Mod. Phys., **30** (1958) 482

[15] NA7 collaboration, S.R. Amendolia et al., Nucl. Phys. **B277** (1986) 168

[16] M.B. Gay Ducati, F. Halzen and A.A.Natale, preprint MAD-PH-750(1993)
F. Halzen, G.I. Krein and A.A. Natale, Phys. Rev. **D47** (1992) 295

[17] J.R. Cudell and D.A. Ross, preprint McGill 92-50

[18] H.C. Cheng and T.T. Wu, *Expanding Protons: Scattering at High Energies* (MIT Press: Cambridge, 1987)

[19] J.E. Mandula and M. Ogilvie, Phys. Lett. **B185** (1987) 127
P.A. Amundsen and J. Greensite, Phys.Lett. **B173** (1986) 179
S.P. Li, Phys. Rev. **D32** (1985) 3321

[20] D. Zwanziger, Nucl. Phys. **B323** (1989) 513

[21] B.U. Nguyen, Ph. D. thesis (1993).

[22] M. Baker, J.S. Ball and F. Zachariasen, Nucl. Phys. **B186** (1981) 531 and references therein

[23] J.R. Cudell, Nucl. Phys. **B336** (1990) 1
A. Donnachie and P.V. Landshoff, Nucl. Phys. **B311** (1989) 509.

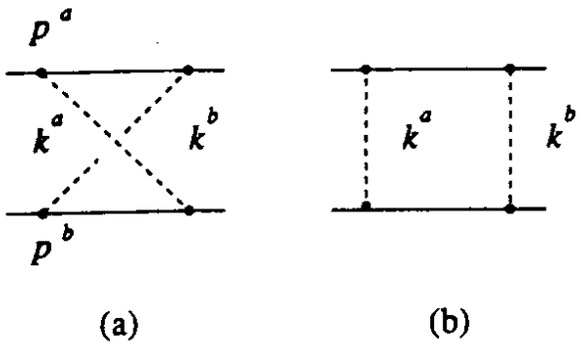

Figure 1

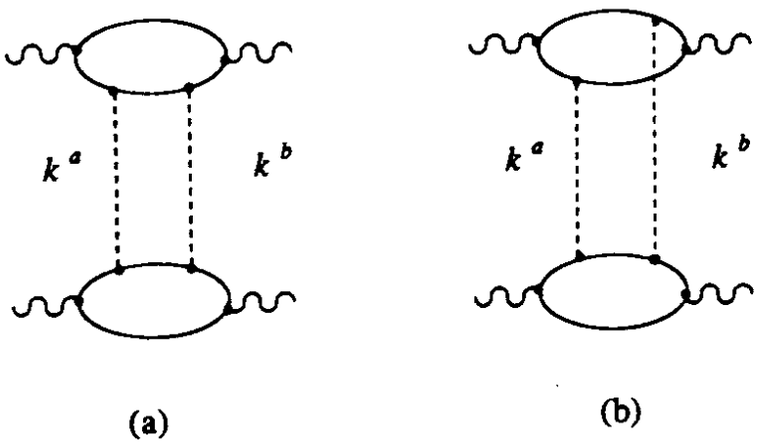

Figure 2

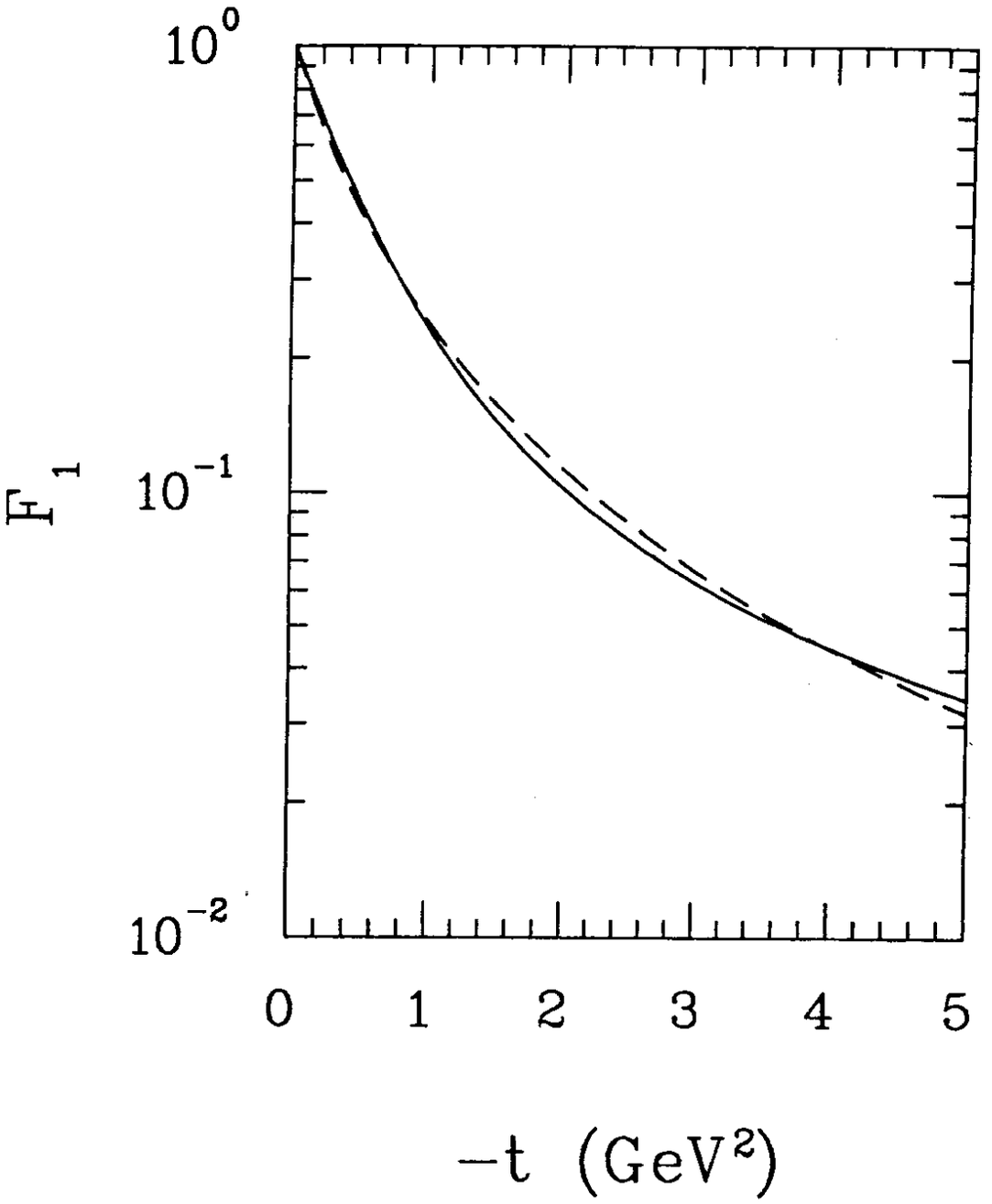

Figure 3

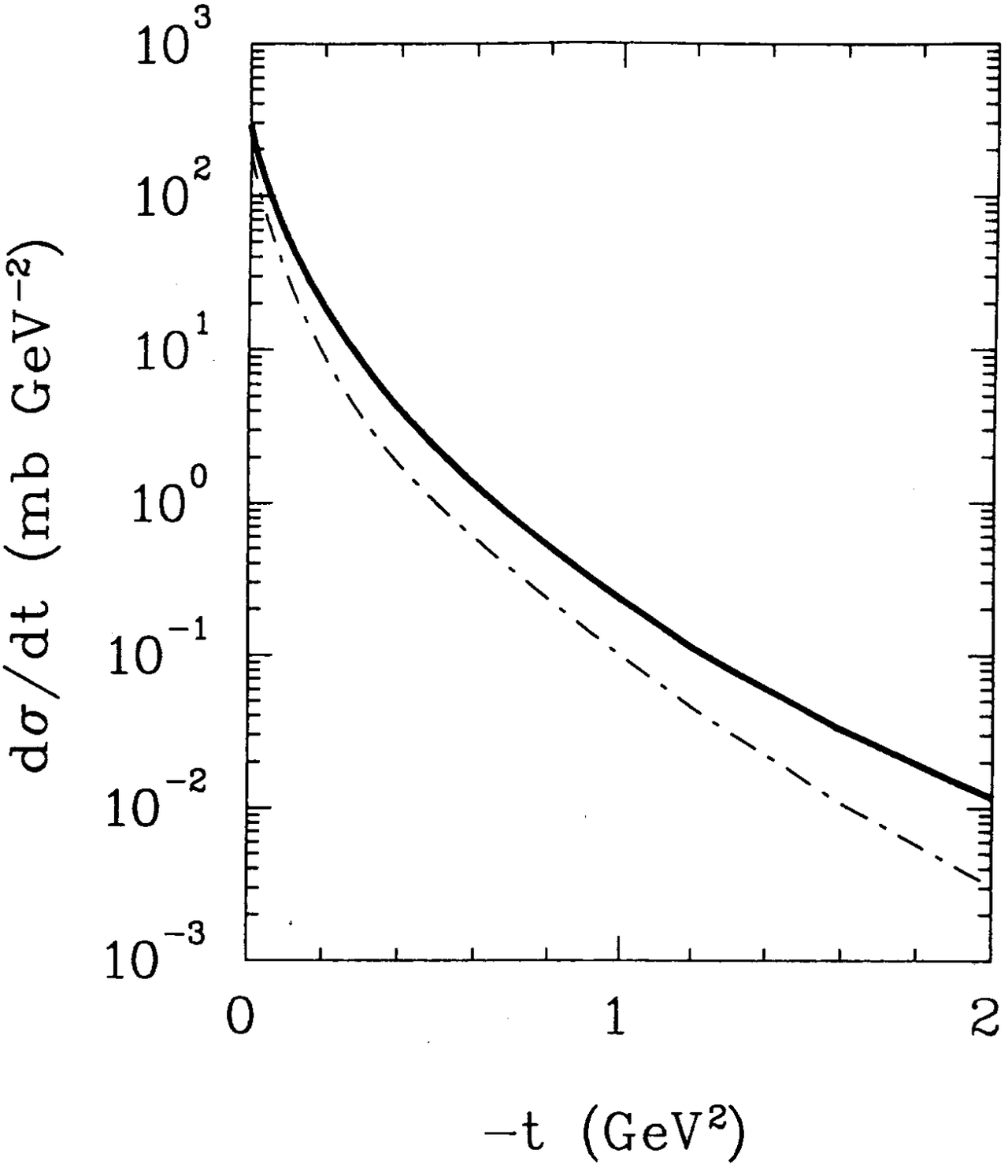

Figure 4

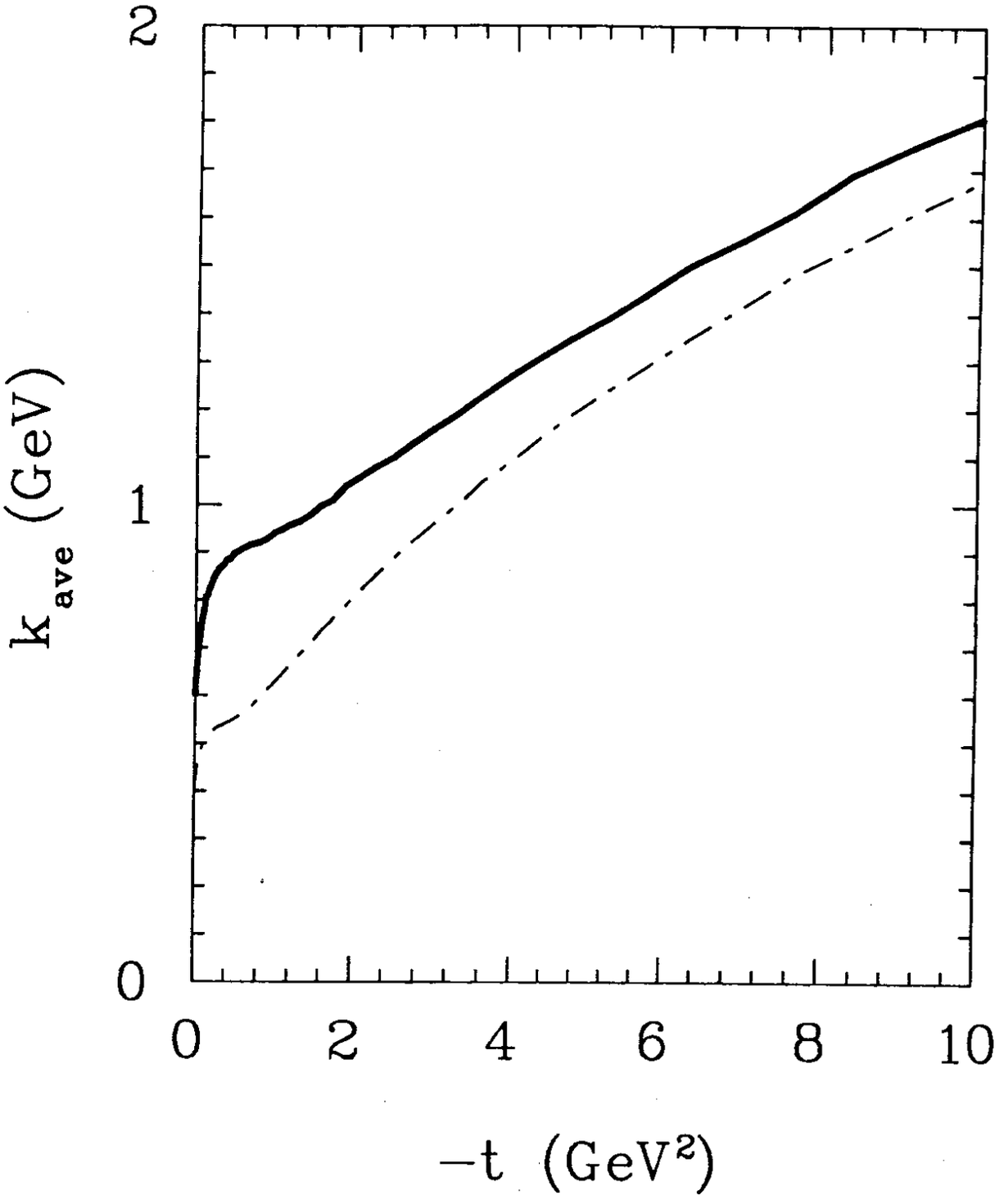

Figure 5

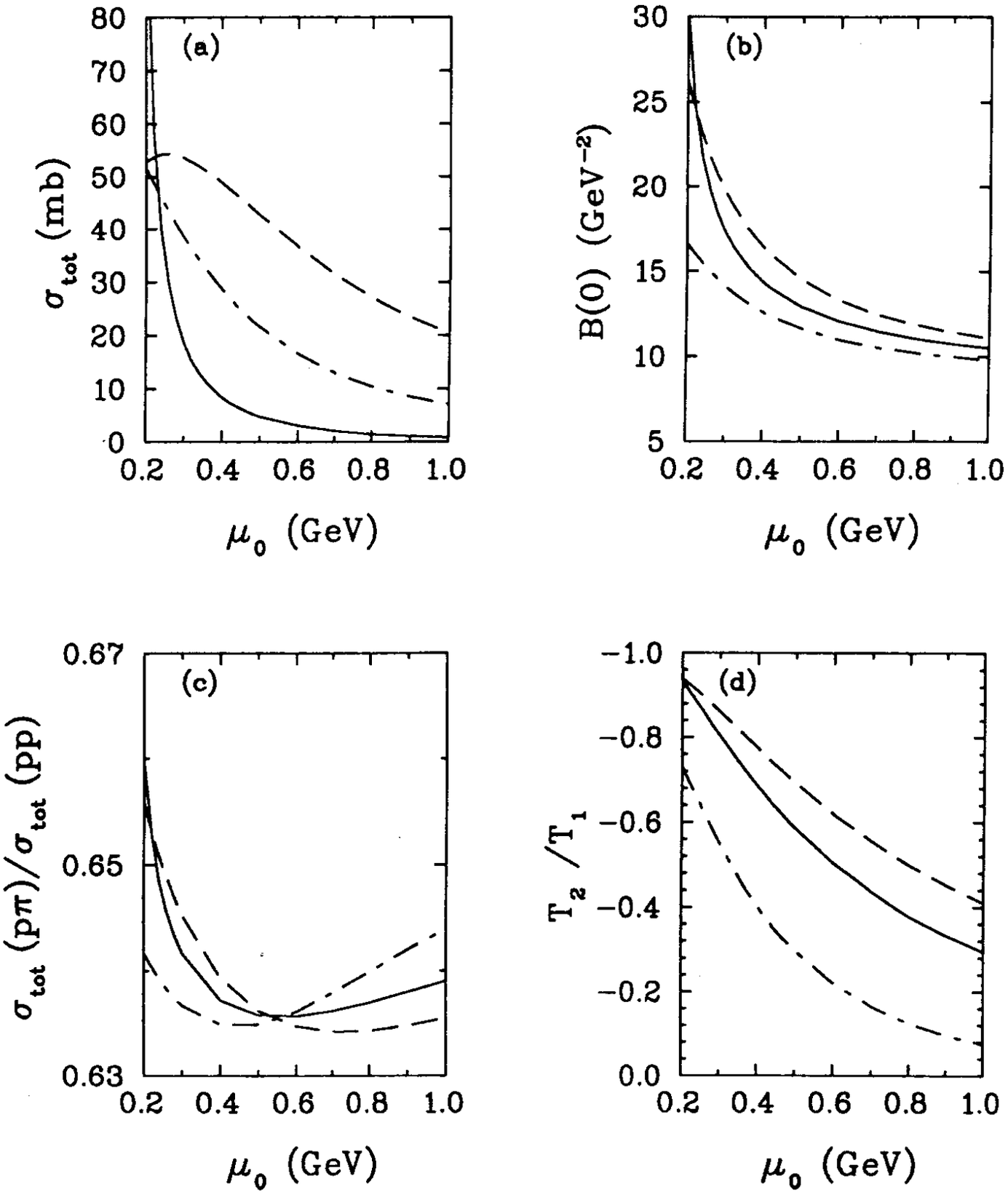
(a)
σ_{tot} (mb)
80
70
60
50
40
30
20
10
0
0.2
0.4
0.6
0.8
1.0
μ_0 (GeV)
(b)
B(0) (GeV^{-2})
30
25
20
15
10
5
0.2
0.4
0.6
0.8
1.0
μ_0 (GeV)
(c)
σ_{tot} (pπ)/σ_{tot} (pp)
0.67
0.65
0.63
0.2
0.4
0.6
0.8
1.0
μ_0 (GeV)
(d)
T_2/T_1
−1.0
−0.8
−0.6
−0.4
−0.2
0.0
0.2
0.4
0.6
0.8
1.0
μ_0 (GeV)

Figure 6

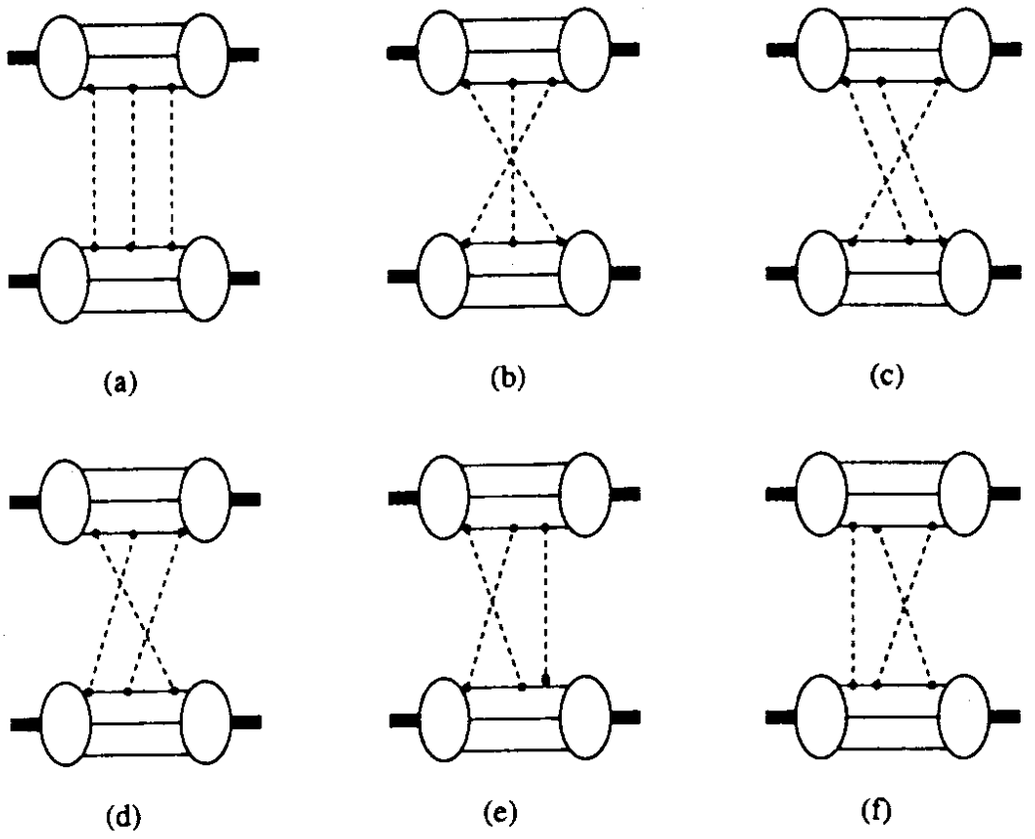

Figure 7

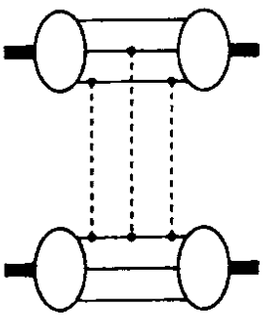

Figure 8

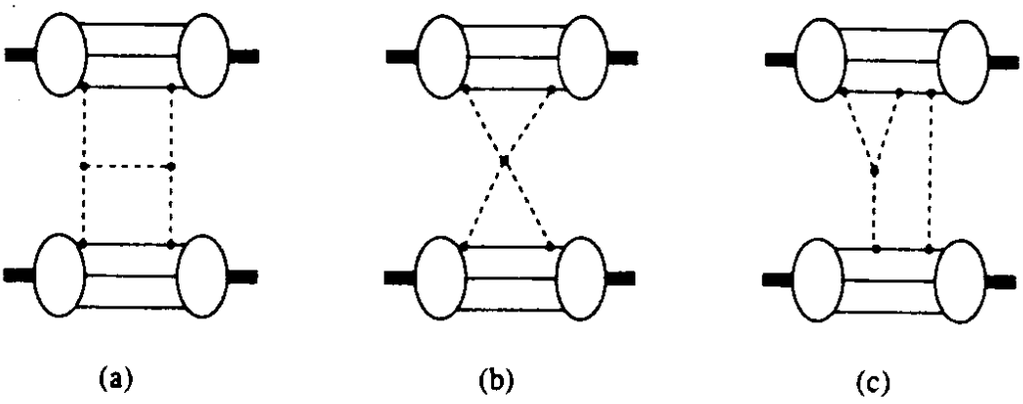

Figure 9

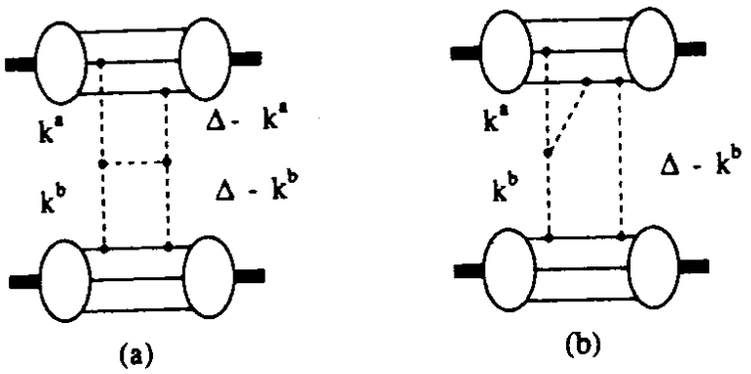

Figure 10

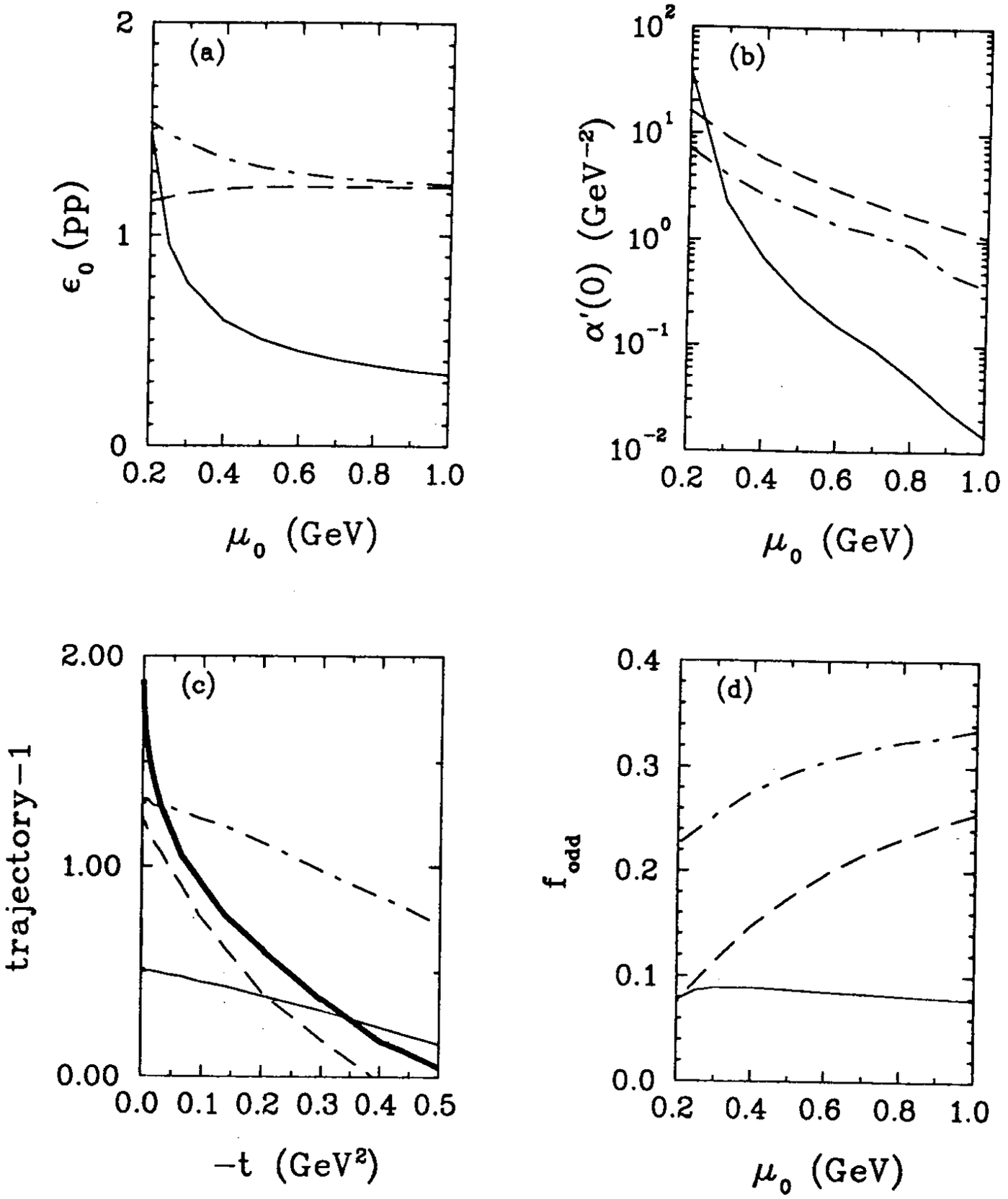
(a)
ϵ_0 (pp)
2
1
0
0.2
0.4
0.6
0.8
1.0
μ_0 (GeV)
(b)
$\alpha'(0)$ (GeV^{-2})
10^2
10^1
10^0
10^{-1}
10^{-2}
0.2
0.4
0.6
0.8
1.0
μ_0 (GeV)
(c)
trajectory-1
2.00
1.00
0.00
0.0
0.1
0.2
0.3
0.4
0.5
$-t$ (GeV^2)
(d)
f_{odd}
0.4
0.3
0.2
0.1
0.0
0.2
0.4
0.6
0.8
1.0
μ_0 (GeV)

Figure 11